# An improved articulated model of the human hand

John McDonald, Jorge Toro,
Karen Alkoby, Andre Berthiaume,
Roymieco Carter,
Pattaraporn Chomwong,
Juliet Christopher,
Mary Jo Davidson,
Jacob Furst, Brian Konie,
Glenn Lancaster,
Lopa Roychoudhuri,
Eric Sedgwick, Noriko Tomuro,
Rosalee Wolfe

School of Computer Science, Telecommunications
and Information Systems, DePaul University,
243 S. Wabash Ave., Chicago, IL 60604, USA
e-mail: asl@cs.depaul.edu

We present an improved anatomically based
approach to modeling the human hand for
use in the animation of the American Sign
Language. The joint rotations in the model
are based on the bone and muscle configu-
rations of the hand, and a forward kinematic
solution is used to position the hand. In par-
ticular, we investigate the rotations of the
base joint of the thumb. This joint is a sad-
dle joint with nontrivial rotational axes and
centers, and must be treated with care in such
a model. We take advantage of several cor-
relations between joint rotations in the hand
to reduce the number of degrees of freedom
in the model and to provide a simple, natural,
and interactive interface for American Sign
Language handshape transcription.

**Key words:** Modeling – Animation – Amer-
ican sign language – Anatomically based
modeling
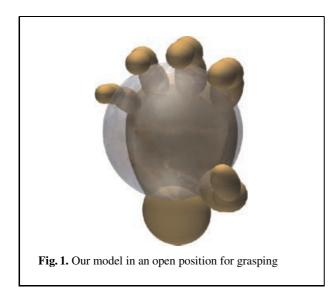
*Correspondence to*: J. McDonald

## 1 Introduction

The present work has arisen out of a need to pro-
duce recognizable animations of the American Sign
Language (ASL). ASL is a natural language used
by members of the North American deaf commu-
nity and is the third or fourth most widely used
language in the United States (Sternberg 1996). At
present, deaf people rely on sign language inter-
preters for access to spoken English, but cost, avail-
ability, and privacy issues make this an awkward
solution at best. A digital sign language interpreter,
which translates spoken English into ASL, would
better bridge the gulf between deaf and hearing
worlds.

Current technology for the translation of written En-
glish includes closed captioning on television. This
is a good first effort at making spoken English more
accessible to the deaf population, but does not repre-
sent a completely satisfactory solution. While ASL
shares some vocabulary with English, there is no
simple word-for-word translation. Further, research
in linguistics shows that ASL's concise and ele-
gant syntax differs radically from English grammar
(Klima and Bellugi 1979; Valli and Luca 1993). Be-
cause of the differences in the two languages, most
native ASL signers read English at the third- or
fourth grade level (Holt 1994). Again, a digital sign
language interpreter, which translates written En-
glish into ASL, would better aid the deaf community.
In ASL, the shape of the hand is a key deter-
minant of a sign's meaning, and the standard for
judging specific handshapes is high. Often a slight
change in a feature of a handshape will render it
unrecognizable.

ASL also presents a need for efficient, realistic tech-
niques for handshape transcriptions for use in ani-
mation. We are building a lexical database for ASL
with the goal of working with a group of native ASL
signers who will transcribe the signs. ASL signers
are not necessarily trained in mathematics or com-
puter graphics, and few are willing to invest the large
amount of time necessary to learn a generalized ani-
mation package.

The human hand, like most articulated figures, can
be modeled as a collection of articulated rigid bod-
ies connected by joints with one or more degrees
of rotational freedom. While the body of work on
articulated figures is large and varied (Badler et al.
1999; Earnshaw et al. 1998; Zhao and Badler 1994),
the number of studies of the hand is relatively small
when compared to the literature on human motion.
When modeling the human figure for ergonomic

**Fig. 1.** Our model in an open position for grasping

studies or for virtual stunt doubles in film, the gross behavior of human motion is the key element, and subtle features like those of the hand can remain simplistic (Badler et al. 1999).

The main body of work in computer animation of the human hand has revolved around the ability of an animated character to grasp objects effectively and convincingly (Rijpkema and Girard 1991). However, the act of grasping does not encompass the full range of expressiveness that a human hand can achieve. This work has limited usefulness for other applications, such as depicting ASL, because the hand is almost always in an open configuration necessary to encompass the object (Fig. 1). Furthermore, the approximation of the thumb used in many grasping models does not accurately reflect the motions of the human thumb (Girard 1990).

Related work in robotics also addresses grasping. However, the main purpose of most robot arms is to manipulate machinery, not to reproduce convincingly the possible shapes of the human hand. Few robotic hands mimic the mechanics of a human hand, and many have fewer than five digits. One notable exception is Jaffe's (1994) work on creating a mechanical finger spelling hand for the deaf-blind.

Other work on modeling the human hand has centered on modeling deformations of both the skin and external objects during a grasping task (Gourret et al. 1989). Realistic skin deformations such as those described by Gourret et al. (1989) are definitely desirable for realism in many applications, but the computational cost of such models is still prohibitive for many real-time animations.

We desired an efficient, anatomically based model of the joints in the human hand that simulates realistic joint rotations and can be manipulated with a natural set of interactive controls. The geometry of the model and the user interface should accurately reflect the basic motions of the human fingers and thumb. Since we were primarily interested in the final shape of the hand, and not in the precise points of contact with other objects, we could use a forward kinematic solution.

As we shall see, the geometry of the joints in the hand must be specified with care to achieve natural motions of the hand while we minimize unneeded degrees of freedom in the model. Our model contains several key improvements, which enhance the hand's expressiveness, preserve the simplicity in the model, and allow for an intuitive interface.
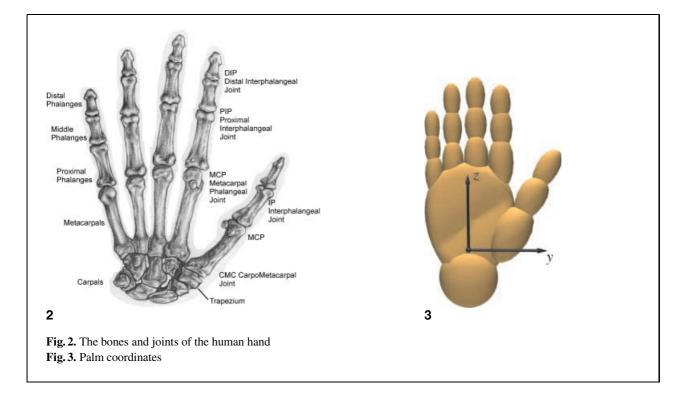
## 2 The anatomy of the human hand

We begin with a short anatomical description of the hand. For a complete description, see Cailliet (1982), Landsmeer (1955), and Netter (1987). The base of the hand consists of a collection of small carpal bones (Fig. 2). Because the motions of these bones are primarily related to the flexion and abduction of the wrist, we ignore most considerations of the carpals in this work with one exception. The carpal that articulates with the base of the thumb is called the trapezium, and its shape has an enormous effect on the motion of the thumb.

The main body of the palm is composed of four long bones called the metacarpals that articulate with the carpals in a collection of joints known as the carpometacarpal (CMC) joints. Each metacarpal bone forms the base of a finger. An additional and far more mobile metacarpal bone forms the base of the thumb, and articulates with the trapezium.

The second and third metacarpal bones, for the index and middle fingers, respectively, are fixed, while the metacarpals of the ring and pinky fingers are free to move in a small range. Metacarpals four and five account for some motion in the fingers and for deformations in the palm itself, but we ignore the contribution of these metacarpals in the present work.

Each finger is composed of three additional bones, the proximal, medial, and distal phalanges. The

**Fig. 2.** The bones and joints of the human hand
**Fig. 3.** Palm coordinates

joint between the metacarpal and the proximal phalange is the metacarpal-phalangeal (MCP) joint. The next joint in the finger is the proximal interphalangeal (PIP) joint and the last joint is the distal interphalangeal (DIP) joint. The interphalangeal joints are hinge joints that allow a small amount of hyperextension, while the MCP joint is more mobile.

The thumb is the most complex subsystem of the hand. The first metacarpal bone in the hand is the base bone of the thumb. This bone articulates with the trapezium in the first CMC joint. The articular surfaces of this joint are both saddle shaped, and a loose, but strong, articular capsule joins the bones. This provides the joint with an axis of motion for flexion and extension as well as an axis for abduction and adduction. The looseness of the joint also allows for a small degree of passive rotary movement in the thumb, enabling opposition (Netter 1987).

Like the other fingers, the thumb also has an MCP joint connecting the metacarpal bone of the thumb to the proximal phalanx, and an interphalangeal (IP) joint that connects the proximal and distal phalanges. Notice that the MCP joint in the thumb is a hinge joint unlike the MCP joints of the fingers, and that the thumb has no middle phalanx.

## 3 Our model

Our representation of the hand consists of 16 articulated rigid bodies, which represent the palm and the bones of the fingers and thumb. For convenience and computational efficiency, we model the palm as a single rigid body. This does not restrict our model unnecessarily, but we do have to introduce some addition rotational freedom in certain joints to compensate.

We place a reference right-handed coordinate frame $M_{\text{palm}}$ in the plane of the palm at its base, with the $z$-axis oriented up toward the fingers, the $y$-axis to the right toward the thumb, and the $x$-axis oriented out of the palm as in Fig. 3.

### 3.1 The fingers

The MCP joints of the fingers have two degrees of freedom about orthogonal axes. We begin with the fingers extended so that the $z$-axes of the fingers are parallel to the $z$-axis of the palm. Number the digits in the hand from one to five beginning with the thumb. Place a local coordinate frame $M_i$ at the base of the proximal phalanx of finger $i$, which is a parallel translation of $M_{\text{palm}}$. The rotations for spreading

and bending the fingers occur about the $x$ and $y$-axes, respectively.

The MCP joints of the fingers are not colinear (Fig. 2), but the specific curve spanned by these joints depends on the hand in question. We position these joints along an arc representing the top of a typical palm. We refine the specifications of this curve momentarily.

There is a small degree of twist about each finger's $z$-axis that occurs automatically in the fingers as they are spread (Cailliet 1982). Since this twist amount is small, we found that by taking a median twist of each finger's coordinate frame to be the default position, we could obtain most of each finger's expressiveness.

Consider that, if the $y$-axes of the bend rotations for all of the fingers are parallel, then when the fingers are bent 90° at the MCP joint, the tips of the fingers will not converge (Fig. 4). The significance of these twists is that they cause the fingers to converge as the MCP joint is bent. Furthermore, if we cause the fingers to twist a bit more as they are spread, we can compensate somewhat for the absence of the metacarpals in the model. Thus, we correlate a $z$-axis twist of the finger with the spreading action, comprising a range of $[-10°, 10°]$ about these default amounts.
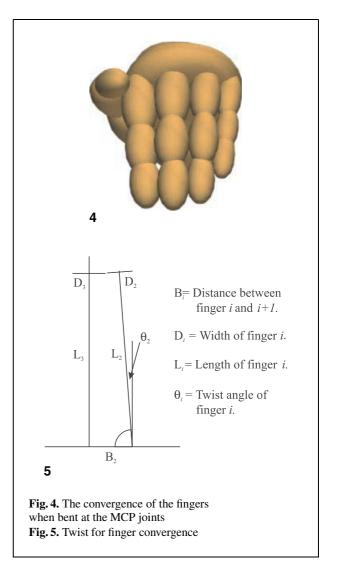
The base twist amount depends on finger length. Let $L_i$ denote the resting lengths of each finger. Let $B_i$ denote the distance between finger $i$ and $i + 1$ at the MCP joint, and let $P_i$ and $D_i$ denote the width of each finger at the PIP and DIP joints, respectively. Since the twist angles of each finger relative to its neighbors are small, the following angles will yield approximate bend convergence in the fingers while avoiding collisions (Fig. 5).

$$\theta_2 = \arcsin\left(\frac{2B_2 - (D_2 + D_3)}{2L_2}\right)$$
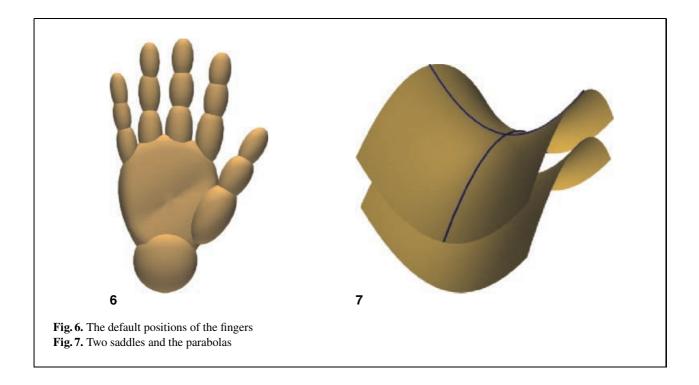
$$\theta_4 = \arcsin\left(\frac{2B_4 - (D_4 + D_3)}{2L_4}\right)$$

$$\theta_5 = \arcsin\left(\frac{2(B_4 + B_3) - (D_5 + 2P_4 + P_3)}{2L_5}\right)$$

and $\theta_3 = 0$. We then position the MCP joints so that they lie on a curve to which these $y$-axes are tangential while their base separations $B_i$ are preserved.



**4**

**5**

$B_i$ = Distance between finger $i$ and $i+1$.

$D_i$ = Width of finger $i$.

$L_i$ = Length of finger $i$.

$\theta_i$ = Twist angle of finger $i$.

**Fig. 4.** The convergence of the fingers when bent at the MCP joints
**Fig. 5.** Twist for finger convergence

Rotation about the MCP joints $y$-axis yields the bending motion of the finger, while rotation about the $x$-axis spreads the finger. We apply the spread rotation first and then the bend rotation to the MCP joint. Unfortunately, the rotational limits for the spread axis are not uniform among the fingers. This is mostly due to the metacarpal bones in the palm. They are not lined up parallel to the $z$-axis of the palm, but rather they radiate out from the wrist at angles of approximately $-8°, 0°, 4°$, and $14°$ for the index, middle, ring, and pinky fingers, respectively (Fig. 6).

Once we rotate the coordinate frames of the MCP joints about their $x$-axes by these amounts, most of the nonuniformities in the spread limits disappear,

**Fig. 6.** The default positions of the fingers
**Fig. 7.** Two saddles and the parabolas

and we can give each of these joints a rotational limit of $[-25°, 30°]$ about the $x$-axis. The bend action in the MCP joint is simpler with a flexion limit of $[0°, 90°]$ and about $15°$ of hyperextension.

The other two joints in the fingers are simpler hinge joints. They have one degree of freedom about their $y$-axes. Experimental evidence shows that, in normal hands, the rotation limits of the PIP joint are generally $[0°, 110°-120°]$. The DIP joint is similar, but only has a range of motion of $[0°, 80°-90°]$. Both the PIP and the DIP joints also have the ability to hyperextend passively for about $15°-25°$ (Cailliet 1982).

## 3.2 The thumb

This brings us to the thumb, the digit that gives our hand much of its expressiveness for applications such as ASL. The thumb is composed of three bones rather than four, but the connection between the trapezium and the metacarpal bone has far more freedom than any of the other joints in the hand.

As mentioned previously, the thumb's CMC joint is a saddle joint with very complex rotations. Both the articular surfaces of the trapezium and the base of the metacarpal roughly form hyperbolic paraboloids.

Such a joint can move along two orthogonal axes, but the foci of the resulting rotations are different (Fig. 7). Movement from a point on a hyperbolic paraboloid can proceed along two orthogonal parabolas: one oriented upwards, the other, downwards, as in the figure. Movement along the upward pointing parabola causes a rotation of the metacarpal with a focus inside the metacarpal itself, whereas movement along the other parabola causes a rotation of the metacarpal with a focus in the trapezium.

The articulation between the trapezium and the metacarpal is quite loose, allowing this joint to rotate passively a bit. Since we did not try to correlate rotations about different foci for this bone, we turned to the muscles of the thumb to determine a simple set of rotations to mimic the thumb's behavior. We place the center of these rotations inside the base of the metacarpal and give the joint some added rotational freedom to compensate for the lack of a true saddle joint here.

The largest muscle for the thumb is the adductor pollicis, which originates along the metacarpals of index and ring fingers, and inserts into the base of the proximal phalanx (Netter 1987). The orientation of this muscle causes a lateral movement of the thumb across the palm upon contraction. Thus, one of the

primary rotations of the thumb is about an axis approximately equal to the $z$-axis of the palm itself. The limits on the motion of the thumb about this axis are approximately $[-25°, 90°]$ including hyperextension. These rotations are measured from the plane of the palm.

With these rotational limits, however, we could not achieve a realistic convergence of the thumb and pinky fingers due to the absence of movement in the fourth and fifth metacarpal bones, and also due to the position of the focus of the rotation. To compensate, we gave the metacarpal bone a rotational limit of 120° about this axis and allowed a small amount of additional rotational freedom in the pinky as already described.

The other motion of the thumb's metacarpal bone is the spread or extension of the thumb. This motion is caused by several muscles along the sides of the thumb, and serves to rotate the thumb away from the vertical axis of the palm. One interesting aspect of this rotation is that, depending on the position of the thumb, the action is caused by different sets of muscles, but this fact does not inconvenience us, as the functional result is the same in any case. This rotation has a functional range of approximately $[10°, 90°]$.

These two rotations reduce the motions of the thumb to rotations along the coordinate axes of a spherical coordinate system based inside the metacarpal. The adduction or bend of the thumb across the palm becomes the traditional rotation of $\theta$ about the vertical axis, and the spread or extension of the thumb becomes the $\phi$ rotation away from this vertical axis.

The last aspect of the thumb's motion that needs consideration is a passive twist of the thumb correlated to the spread action. This twist places the thumb in certain positions of opposition. If one places the thumb in front of the palm and vertically in line with the index finger, and then spreads the thumb away from the palm, one will notice that the thumb passively rotates about its $z$-axis during the extension (Cailliet 1982; Netter 1987).

To model this twist in the thumb, we placed a rotational correlation between the spread of the thumb and a twist about the thumb's local $z$-axis. This twist begins when the thumb is spread by approximately 60% of its range and encompasses approximately 45° of rotation. We also scale this rotation in the case where the bend angle $\theta$ of the thumb is less than about 20°, in accordance with our observation

that the thumb does not twist as much during spread when it is in these positions.

### 3.3 Other rotational correlations

Fortunately, this twist in the thumb is not the only correlation between rotations in the hand. We have already noted the correlation between the spread of the fingers and a small twist about their $z$-axes. In addition, there is a far more noticeable correlation between the DIP and PIP joints in the fingers for hooking actions. As has been observed in previous works (Landsmeer 1958; Rijpkema and Girard 1991), the tendons that bend the DIP joint also bend the PIP joint. In most hooking actions of the fingers, such as during grasping, the DIP bend is approximately 2/3 that of the PIP (Rijpkema and Girard 1991). We isolate this rotational correlation as an independent action called the hook of the finger.

There is also independent motion in the PIP joint itself, but unless the MCP joint of the finger is fully bent, this motion is difficult to achieve, so we restrict this motion to the case when the MCP joint is fully bent. Thus, we can merge two independent aspects of the bending of the finger into one degree of freedom. The bend of the finger begins with a rotation of the MCP joint about its $y$-axis until it is bent at 90°. The motion then proceeds by bending the PIP joint independently of the DIP joint from 0° to 90°–110°, depending on the flexibility of the hand in question.

In their recent paper on a general 3D model of the human hand, Ouhaddi and Horain (1998) describe other rotational correlations in the hand that may be useful in future models. However, we found that the correlations just described gave us the realism and simplicity needed for ASL.

## 4 Rotational controls for the hand

We take advantage of the rotational correlation in the user interface of our handshape transcription system. ASL linguists have identified several key independent motions in the fingers that are significant for ASL (Brentari 1998; Liddell and Johnson 1989; Sandler 1989), and fortunately, these motions correspond well to the rotational correlations we have specified. The fingers have three independent degrees of freedom. The following list

contains a description of each action. Each rotation is taken to vary along the full range of motion specified.

1. Spread: rotation of the MCP joint about its $x$-axis, with the small associated twist in the MCP joint about its $z$-axis.
2. Bend: for half of the bend range, this corresponds to rotation of the MCP joint about its $y$-axis and for the rest of the bend range. It corresponds to rotation of the PIP joint about its $y$-axis.
3. Hook: bending the PIP and DIP joints simultaneously so that the PIP is 3/2 of the DIP, or in other words, the DIP = 2/3 PIP.

Notice that the PIP joint is overspecified by these actions, so for any [Spread, Bend, Hook] triple, we set the PIP joint to the maximum rotation specified by the bend and the hook values.

The thumb has four independent degrees of freedom since the MCP and the DIP joints of the thumb are not correlated, and because the twist of the MCP joint is correlated to the other rotations of the CMC joint of the thumb.

1. Spread: the abduction or extension of the thumb away from the $z$-axis of the palm with the associated twist about the $z$-axis of the thumb
2. Bend: the rotation of the thumb about the $z$-axis of the palm
3. MCP bend: Rotation of the thumb's MCP joint about its $y$-axis
4. DIP bend: Rotation of the thumb's DIP joint about its $y$-axis

With these simple and natural controls, we can place the fingers of the palm in the positions necessary for ASL, and animations of the handshapes look natural and convincing.

We implemented our version of the hand transcriber with a commercially available animation package, and we used that package's scripting language to implement the rotational controls and constraints. The simplicity of its interface makes it feasible for laymen to use it effectively. In the Appendix, we present a collection of pictures of a human hand making various ASL handshapes along with their representations in our model.

## 5 Conclusions and future work

Our model provides a natural interface for shaping the positions of the fingers in the hand for ASL and many other applications. Initial user tests within the deaf community have been very promising, as it took only a few minutes for test subjects to familiarize themselves with the interface and then less than 2 min for them to transcribe a handshape such as ASL's "m" or "t".

This model still has one main deficiency that does not hinder its effectiveness for ASL. The absence of the metacarpal bones for the pinky and ring fingers makes it difficult to place the hand in certain configurations where the thumb is touching the pinky. Thus, we must make the palm deformable and add support for these two bones in the model and interface.

The next major improvement for this model would then be to transform the palm and fingers into deformable surfaces and to model the underlying bones and musculature of the hand to give it a far more realistic appearance as in Wilhelms and Van Gelder (1997), Gourret et al. (1989), and Scheepers et al. (1997).

## References

1. Badler N, Palmer M, Bindiganavale R (1999) Animation control for real-time virtual humans. Commun ACM 42:64–73
2. Brentari D (1998) A prosodic model of sign language phonology. MIT Press, Cambridge, Mass
3. Cailliet R (1982) Hand pain and impairment, 3rd edn. F.A. Davis, Philadelphia, Penn
4. Earnshaw R, Magnenat-Thalmann N, Terzopoulos D, Thalmann D (1998) Computer animation for virtual humans. IEEE Comput Graph Appl 18:20–23
5. Girard M (1990) Constrained optimization of articulated animal movement in computer animations, making them move (mechanics, control, and animation of articulated fingers). Morgan Kaufmann, San Francisco, CA
6. Gourret J, Magnenat-Thalmann N, Thalmann D (1989) Simulation of object and human skin deformations in a grasping task. Comput Graph 23:21–30
7. Holt J (1994) Stanford achievement test – 8th edition for deaf and hard of hearing students: reading comprehension subgroup results. http://gri.gallaudet.edu/
8. Jaffe D (1994) Evolution of mechanical fingerspelling hands for people who are deaf-blind. J Rehabilitation Research Development 31(3):236–44
9. Klima E, Bellugi U (1979) The signs of language. Harvard University Press, Cambridge, MA
10. Landsmeer J (1958) A report on the co-ordination of the interphalangeal joints of the human finger and its disturbances. Acta Morphologica Neerlando-Scandinavica 2:59–84

11. Landsmeer J (1963) The coordination of finger-joint motions. J Bone Joint Surg 45-A:1654–1662
12. Landsmeer J (1955) Anatomical and functional investigations on the articulation of the human fingers. Acta Anatommica 24 supl 2, 25:1–69
13. Liddell S, Johnson R (1989) American sign language: the phonological base. Sign Language Studies 64:195–277
14. Netter F (1987) The CIBA collection of medical illustrations, vol. 8. Musculoskeletal System. Ciba-Geigy, Tom's River, New Jersey
15. Ouhaddi H, Horain P (1998) Conception et adjustement d'un modèle 3D articulé de la main. Actes des 6èmes journées du Groupe de Travail Réalité Virtuelle, Issy-les-Moulineaux, France, 12/13:83–90
16. Rijpkema H, Girard M (1991) Computer animation of knowledge-based human grasping. Comput Graph 25:339–348
17. Sandler W (1989) Phonological representation of the sign: linearity and nonlinearity in American sign language. Foris Publications, Dordrecht, The Netherlands
18. Scheepers F, Parent R, Carlson W, May S (1997) Anatomy-based modeling of the human musculature. SIGGRAPH '97 Conference Proceedings, Computer Graphics Annual Conference Series, pp 163–172
19. Sternberg M (1996) The American sign language dictionary. Multicom (CD ROM), Seattle, WA
20. Valli C, Luca C (1993) Linguistics of American sign language. Gallaudet University Press
21. Wilhelms J, Van Gelder A (1997) Anatomically based modeling. SIGGRAPH '97 Conference Proceedings, Computer Graphics Annual Conference Series, pp 173–180
22. Zhao Z, Badler N (1994) Inverse kinematics positioning using nonlinear programming for highly articulated figures. ACM Trans Graph 13:313–336

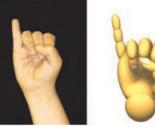# Appendix: Handshape examples



The letter D



The letter E



The letter I



The letter M



The letter N



The letter T



The letter R



The letter S

JOHN MCDONALD earned his PhD in Mathematics from Northwestern University in 1996. He currently holds an assistant professorship at DePaul University's School of CTI. His interests include physically based modeling and simulation, graphics and animation, and computational geometry. He is also part of DePaul University's American Sign Language Team. Composed of hearing and deaf students, and faculty from a wide number of disciplines, the ASL Team's goal is to help bridge the communication gap between the deaf and hearing worlds.

Shown in the picture, left to right, are Pattaraporn Chomwong, John McDonald, and Jorge Toro.